Holographic Magnetism

Rong-Gen Cai (蔡荣根）
Institute of Theoretical Physics
Chinese Academy of Sciences

Refs:

arXiv: 1404.2856, 1404.7737, 1410.5080, 1501.04481,
1504. 00855, 1505.03405, 1507.00546, 1507.03105，
1706.01470 with Y. Q. Yang, F. Kunsmartsev,
Y.B. Wu, C.Y. Zhang, Li Li, Y. Q, Wang and Y. Zaanen

Brief Introduction to ITP

ITP was established in 1978, currently it has 42 faculties, focus on studies in theoretical physics and relevant interdisciplinary fields.

- Theoretical particle physics and nuclear physics
- String theory and quantum field theory
- Gravitational theory, astrophysics and cosmology
- Condensed matter theory
- Statistical physics, theoretical biophysics and bioinformatic
- Quantum physics, quantum information and interaction between light and matter

All are welcome to ITP!

Black hole is a window to quantum gravity

Thermodynamics of black hole

$$\boxed{T = \frac{\hbar k}{2\pi}}$$

$$\boxed{S = \frac{A}{4G\hbar}}$$

S.Hawking, 1974, J. Bekenstein, 1973

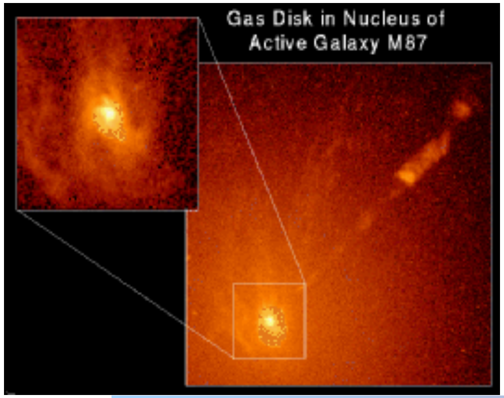

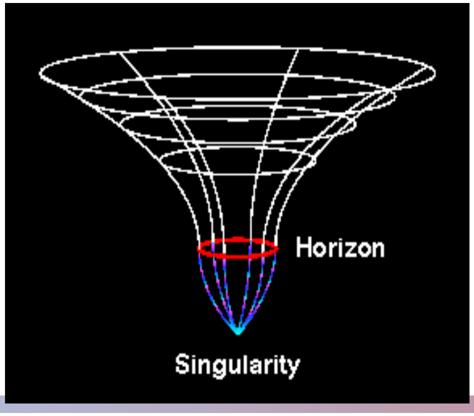

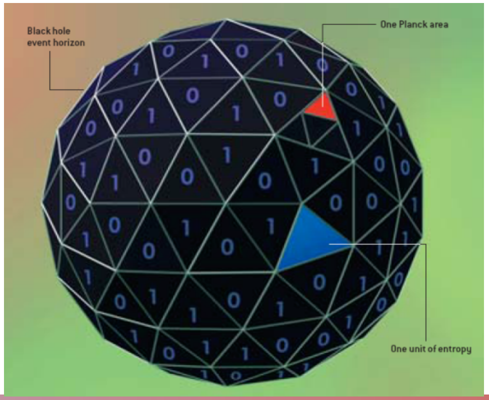

Holography of Gravity

Entropy in a system with surface area A : $S < A/4G$

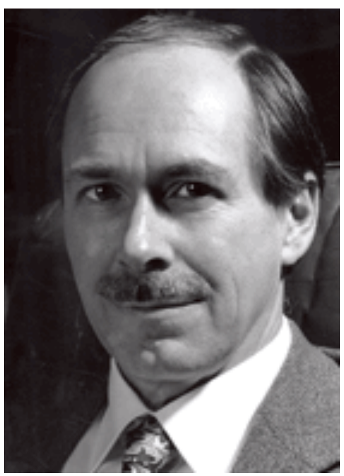

(G. t' Hooft)

(L. Susskind)

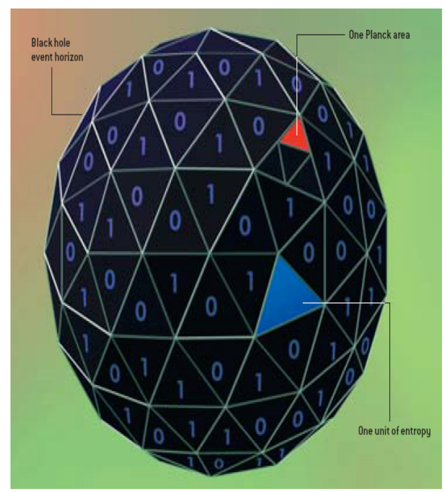

The world is a hologram?

Why GR?

The planar black hole with AdS radius L=1:

$$ds^2 = -r^2[f(r)dt^2 + dx^2 + dy^2] + \frac{dr^2}{r^2 f(r)}$$

where: $f(r) = 1 - \frac{r_+^3}{r^3}$

(1) Temperature of the black hole: $T \sim r_+$
(2) Energy of the black hole: $E \sim r_+^3 V \sim T^3 V$
(3) Entropy of the black hole: $S \sim r_+^2 V \sim T^2 V$

The black hole behaves like a thermal gas in 2+1 dimensions in thermodynamics!

Topology theorem of black hole horizon :

PHYSICAL REVIEW D VOLUME 54, NUMBER 8 15 OCTOBER 1996

Black plane solutions in four-dimensional spacetimes

Rong-Gen Cai* and Yuan-Zhong Zhang
China Center of Advanced Science and Technology (World Laboratory), P.O. Box 8730, Beijing 100080, China
and Institute of Theoretical Physics, Academia Sinica, P.O. Box 2735, Beijing 100080, China

(Received 7 June 1996)

The static, plane symmetric solutions and cylindrically symmetric solutions of Einstein-Maxwell equations with a negative cosmological constant are investigated. These black configurations are asymptotically anti–de Sitter–type not only in the transverse directions, but also in the membrane or string directions. Their causal structure is similar to that of Reissner-Nordström black holes, but their Hawking temperature goes with $M^{1/3}$, where M is the ADM mass density. We also discuss the static plane solutions in Einstein-Maxwell-dilaton gravity with a Liouville-type dilaton potential. The presence of the dilaton field changes drastically the structure of solutions. They are asymptotically "anti–de Sitter–" or "de Sitter-type" depending on the parameters in the theory. [S0556-2821(96)03820-9]

PACS number(s): 04.20.Jb, 04.70.Dy

$$ds^2 = -A(r)dt^2 + B(r)dr^2 + C(r)(dx^2 + dy^2), \qquad (8)$$

$$A(r) = B^{-1}(r) = \alpha^2 r^2 - \frac{m}{r} + \frac{q^2}{r^2},$$

$$C(r) = \alpha^2 r^2,$$

AdS/CFT correspondence（1997, J. Maldacena）：

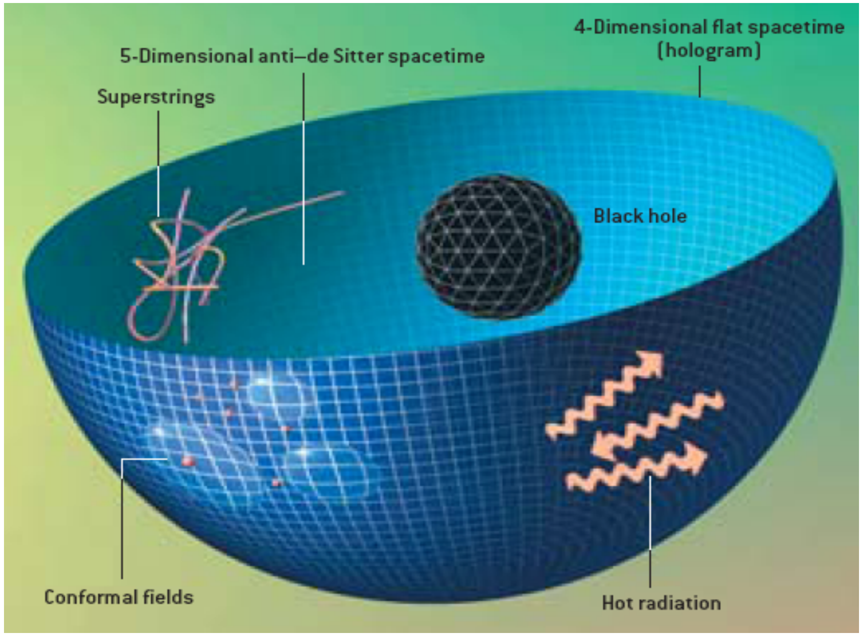

$$Z_{AdS}(\phi_{0,i}) = Z_{CFT}(\phi_{0,i})$$

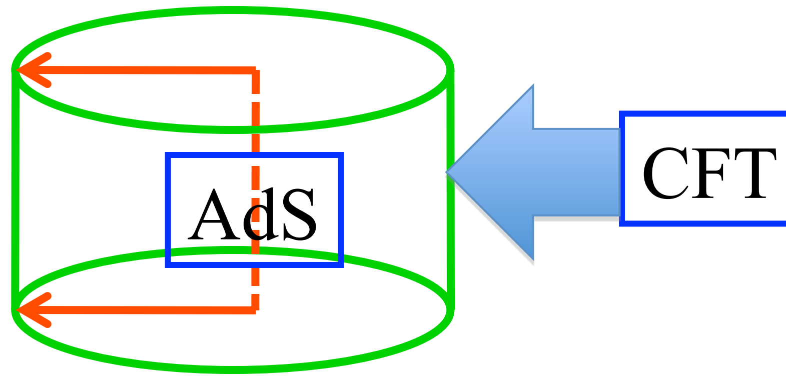

"*Real conceptual change*

in our thinking about Gravity."

（E. Witten, Science 285 (1999) 512

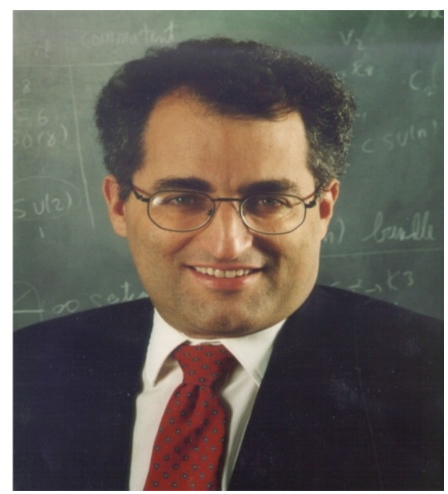

AdS/CFT dictionary :

$$Z_{AdS}(\phi_{0,i}) = Z_{CFT}(\phi_{0,i})$$

$$e^{-I_{AdS}(\phi_i)} = \left\langle e^{\int \phi_{0,i} \mathcal{O}^i} \right\rangle_{CFT}$$

Here $\phi_{0,i}$

in the bulk:

the boundary value of the field propagating in the bulk

in the boundary theory:

the source of the operator dual to the bulk field

Quantum field theory in d-dimensions

quantum gravitational theory in (d+1)-dimensions

operator *O*
boundary

dynamical field ϕ
bulk

energy momentum tensor: $T^{\mu\nu}$		graviton: g_{ab}
global current: J^{μ}		Maxwell field: A_a
scalar operator: $\mathcal{O}_B$	$\leftrightsquigarrow$	scalar field: ϕ
fermionic operator: $\mathcal{O}_F$		fermionic field: ψ .

$$Z_{\text{bulk}}[\phi \to \delta\phi_{(0)}] = \left\langle \exp\left(i \int d^d x \delta\phi_{(0)} \mathcal{O} \right) \right\rangle_{\text{QFT}} .$$

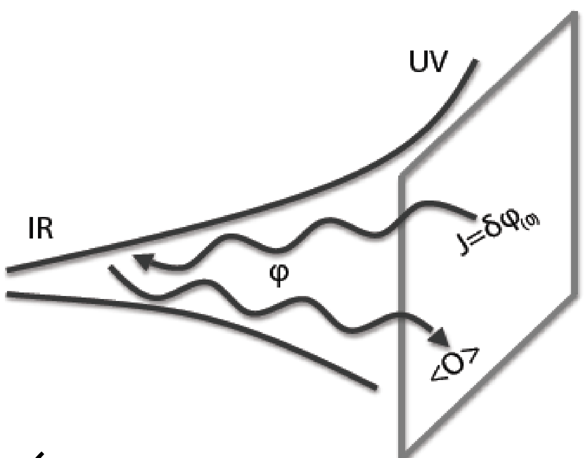

(0909.3553, S. Hartnoll

AdS/CFT correspondence：

1)gravity/gauge field
2) different spacetime dimension
3) weak/strong duality
4) classical/quantum

Applications in various fields:
low energy QCD (AdS/QCD),
condensed matter theory (AdS/CMT)
e.g., holographic superconductivity
(non-) Fermion fluid

Holographic magnetism:

1) Paramagnetism-Ferromagnetism Phase Transition in a Dyonic Black Hole
   Phys. Rev. D 90, 081901 (2014) (Rapid Communication)
2) Model for Paramagnetism/antiferromagnetism Phase Transition
   Phys. Rev. D 91, 086001 (2015)
3) Coexistence and competition of ferromagnetism and p-wave superconductivity in holographic model
   Phys. Rev. D 91, 026001 (2015)
4) Holographic model for antiferromagnetic quantum phase transition induced by magnetic field
   Phys. Rev. D 92, 086001 (2015)
5) Antisymmetric tensor field and spontaneous magnetization in holographic duality
   Phys. Rev. D 92, 046001 (2015)
6) Holographic antiferromganetic quantum criticality and AdS_2 scaling limit
   Phys. Rev. D 92, 046005 (2015)
7) Massive 2-form field and holographic ferromagnetic phase transition
   JHEP 1511 (2015) 021
8) Insulator/metal phase transition and colossal magnetoresistance in holographic model
   Phys.Rev.D92 (2015)106002
9）Intertwined orders and holography: pair density waves : PRL (2017)

Outline:

1 Introduction: holographic superconductor model
2 Ferromagnetism/paramagnetism phase transition
3 Antiferromagnetism/paramagnetism phase transition
4 Antiferromagnetic quantum phase transition
5 Insulator/metal phase transition and colossal magnetoresistance effect
6 Coexistence and competition between ferromagnetism and superconductivity
7 Intertwined orders and holography: the case of the parity breaking pair density wave
8 Summary

how to build a holographic model of superconductors

CFT	CFT/AdS →	Gravity
Global symmetry		Abelian gauge field
Scalar operator		Scalar field
Temperature		Black hole
Phase transition		High T/no hair Low T/ hairy BH

G.T. Horowitz, 1002.1722

Holographic superconductors

Building a holographic superconductor

S. Hartnoll, C.P. Herzog and G. Horowitz, arXiv: 0803.3295

PRL 101, 031601 (2008)

$$16\pi G_N \mathcal{L} = R - \frac{6}{L^2} - \frac{1}{4}F_{\mu\nu}^2 - |\partial_\mu\psi - iqA_\mu\psi|^2 - m^2|\psi|^2 ,$$

High Temperature (black hole without hair):

$$ds^2 = -f(r)dt^2 + \frac{dr^2}{f(r)} + r^2(dx^2 + dy^2) ,$$

$$f = \frac{r^2}{L^2} - \frac{M}{r} .$$

Consider the case of m^2L^2=-2 , like a conformal scalar field.

In the probe limit and A_t= Phi

Taking a plane symmetric ansatz, $\Psi = \Psi(r)$, the scalar field equation of motion is

$$\Psi'' + \left(\frac{f'}{f} + \frac{2}{r}\right)\Psi' + \frac{\Phi^2}{f^2}\Psi + \frac{2}{L^2 f}\Psi = 0\,,$$

$$\Phi'' + \frac{2}{r}\Phi' - \frac{2\Psi^2}{f}\Phi = 0\,,$$

At the large r boundary:

$$\Psi = \frac{\Psi^{(1)}}{r} + \frac{\Psi^{(2)}}{r^2} + \cdots\,.$$

$$\Phi = \mu - \frac{\rho}{r} + \cdots\,.$$

Scalar operator condensate O_i:

$$\langle \mathcal{O}_i \rangle = \sqrt{2}\Psi^{(i)}\,, \quad i = 1, 2$$

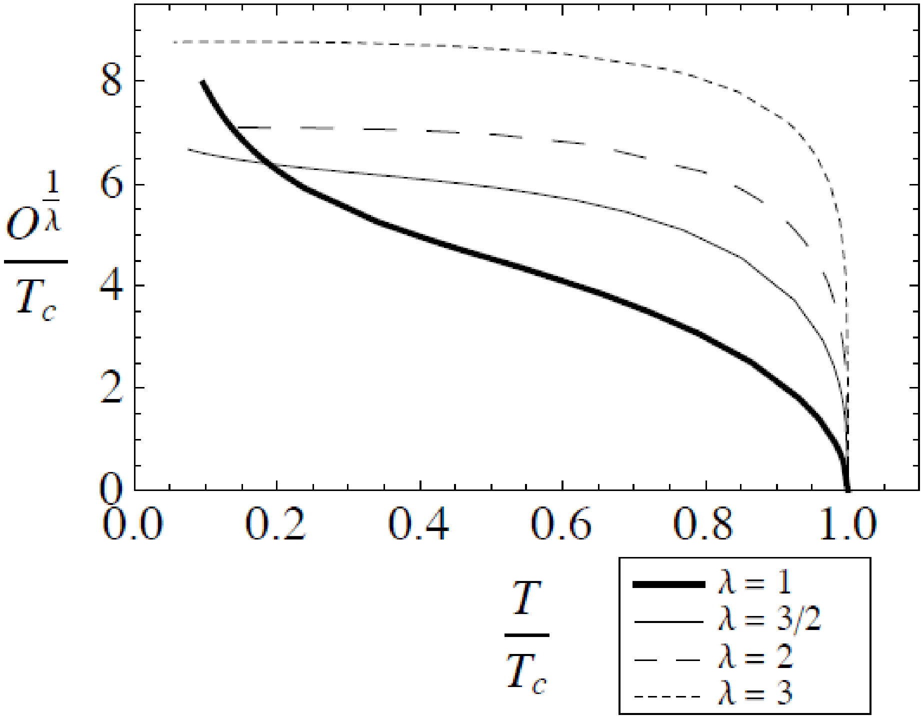

$$\langle \mathcal{O}_1 \rangle \approx 9.3\, T_c\, (1 - T/T_c)^{1/2}\,, \quad \text{as} \quad T \to T_c\,,$$

$$\langle \mathcal{O}_2 \rangle \approx 144\, T_c^2\, (1 - T/T_c)^{1/2}\,, \quad \text{as} \quad T \to T_c\,,$$

Conductivity

Maxwell equation with zero momentum :

$$A_x'' + \frac{f'}{f} A_x' + \left(\frac{\omega^2}{f^2} - \frac{2\Psi^2}{f}\right) A_x = 0\,.$$

Boundary conduction:
at the horizon: ingoing mode
at the infinity:

$$A_x = A_x^{(0)} + \frac{A_x^{(1)}}{r} + \cdots$$

$\Downarrow$ AdS/CFT

source: $A_x = A_x^{(0)}\,, \qquad \langle J_x \rangle = A_x^{(1)}\,.$ current

Conductivity: $$\sigma(\omega) = \frac{\langle J_x \rangle}{E_x} = -\frac{\langle J_x \rangle}{\dot{A}_x} = -\frac{i\langle J_x \rangle}{\omega A_x} = -\frac{iA_x^{(1)}}{\omega A_x^{(0)}}\,.$$

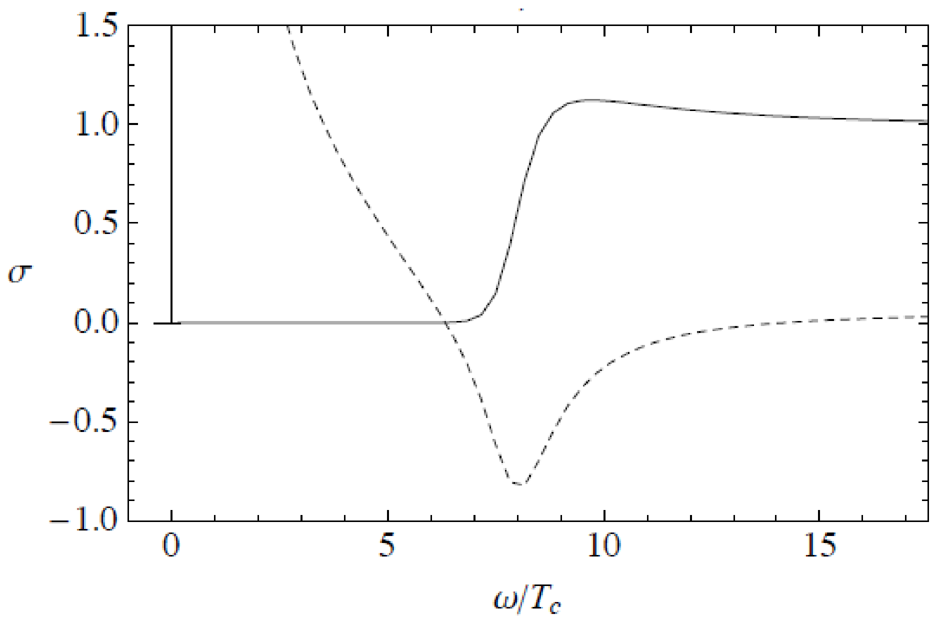

A universal energy gap: ~ 10%

$$\frac{\omega_g}{T_c} \approx 8$$

- BCS theory: 3.5
- K. Gomes et al, Nature 447, 569 (2007)

$Bi_2Sr_2CaCu_2O_{8+\delta}$

Summary:

1. The CFT has a global abelian symmetry corresponding a massless gauge field propagating in the bulk AdS space.

2. Also require an operator in the CFT that corresponds to a scalar field that is charged with respect to this gauge field..

3. Adding a black hole to the AdS describes the CFT at finite temperature.

4. Looks for cases where there are high temperature black hole solutions with no charged scalar hair, but below some critical temperature black hole solutions with charged scalar hair and dominates the free energy.

arXiv: 1003.0010, PRD82 (2010) 045002

March 4, 2010

Quantum phase transitions in holographic models of magnetism and superconductors

Nabil Iqbal,[1] Hong Liu,[1] Márk Mezei,[1] and Qimiao Si[2]

[1] *Center for Theoretical Physics, Massachusetts Institute of Technology, Cambridge, MA 02139*
[2] *Department of Physics and Astronomy, Rice University, Houston, TX 77005*

We study a holographic model realizing an "antiferromagnetic" phase in which a global $SU(2)$ symmetry representing spin is broken down to a $U(1)$ by the presence of a finite electric charge density. This involves the condensation of a neutral scalar field in a charged AdS black hole. We observe that the phase transition for both neutral and charged (as in the standard holographic superconductor) order parameters can be driven to zero temperature by a tuning of the UV conformal dimension of the order parameter, resulting in a quantum phase transition of the Berezinskii-Kosterlitz-Thouless type. We also characterize the antiferromagnetic phase and an externally forced ferromagnetic phase by showing that they contain the expected spin waves with linear and quadratic dispersions respectively.

$$\frac{2\kappa^2}{R^2}\mathcal{L}_{\text{matter}} = -\frac{1}{4g_A^2}F^a_{MN}F^{MNa} - G_{MN}G^{MN} - \frac{1}{\lambda}\left(\frac{1}{2}(D\phi^a)^2 - V(\phi^a)\right) \qquad (54)$$

$$V(\phi^a) = \frac{1}{2}m^2\vec{\phi}\cdot\vec{\phi} + \frac{1}{4}(\vec{\phi}\cdot\vec{\phi})^2 \ .$$

Breaking a global SU(2) symmetry representing spin into a U(1) subgroup. The symmetry breaking is triggered by condensation of a triplet scalar field. This model leads to the spatial rotational symmetry breaking spontaneously, the time reversal symmetry is not broken spontaneously in the magnetic ordered phase.

2、A model for ferromagnetism/paramagnetism transition

arXiv: 1404.2856, PRD 90 (2014) 081901, Rapid Comm.

The model:

$$S=\frac{1}{2\kappa^2}\int d^4x\sqrt{-g}(R+\frac{6}{L^2}-F^{\mu\nu}F_{\mu\nu}-4j^\mu A_\mu+\lambda^2 L_M) \tag{1}$$

where

$$\begin{aligned} L_M = & -\frac{1}{4}\nabla^\mu M^{\nu\tau}\nabla_\mu M_{\nu\tau}-\frac{m^2}{4}M^{\mu\nu}M_{\mu\nu} \\ & -\frac{1}{2}M^{\mu\nu}F_{\mu\nu}-\frac{J}{8}V(M_{\mu\nu}). \end{aligned} \tag{2}$$

$$V(M_{\mu\nu})=M_\mu{}^\nu M_\nu{}^\tau M_\tau{}^\delta M_\delta{}^\mu$$

The reasons:

1)The ferromagnetic transition breaks the time reversal symmetry, spatial rotating symmetry, but is not associated with any symmetry such as U(1), SU(2).

2)The magnetic moment is a spatial component of a tensor,

3) In weak external magnetic field, it is proportional to external magnetic field.

We are considering the probe limit, the background is

$$ds^2 = r^2(-f(r)dt^2 + dx^2 + dy^2) + \frac{dr^2}{r^2 f(r)},$$
$$f(r) = 1 - \frac{1+\mu^2+B^2}{r^3} + \frac{\mu^2+B^2}{r^4},$$
$$A_\mu = \mu(1-1/r)dt + Bxdy,$$

Temperature: $T = (3-\mu^2-B^2)/4\pi.$

The ansatz: $M_{\mu\nu} = -p(r)dt \wedge dr + \rho(r)dx \wedge dy.$

$$\rho'' + \frac{f'\rho'}{f} - \left(\frac{2f'}{f} + \frac{4}{r^2} + \frac{m^2}{r^2 f}\right)\rho + \frac{J\rho^3}{r^6 f} - \frac{B}{r^2 f} = 0,$$
$$p'' + \left(\frac{f'}{f} + \frac{4}{r}\right)p' - \left(\frac{2}{r^2} + \frac{m^2}{r^2 f}\right)p - \frac{Jp^3}{r^2 f} - \frac{\mu}{r^4 f} = 0, \tag{8}$$

The boundary condition:

$$\rho' = 2\rho - \frac{\rho(J\rho^2 - m^2) - B}{4\pi T},$$
$$p' = \frac{Jp^3 + m^2 p - \mu}{4\pi T}.$$

$$\rho \sim \rho_+ r^{(1+\delta)/2} + \rho_- r^{(1-\delta)/2} - \frac{B}{4+m^2},$$
$$p \sim p_+ r^{(-3+\delta)/2} + p_- r^{(-3-\delta)/2} - \frac{\mu}{(4+m^2)r^2},$$
$$\delta = \sqrt{17+4m^2}.$$

On the other hand, in order to the condensate happens spontaneously when the temperature is lowered, the m^2 of the real tensor field should violate the BF bound of the field in $AdS_2 \times R^2$. This leads to the constraint of m^2 as

$$-4 < m^2 < -\frac{3}{2}. \qquad (13)$$

The off-shell free energy:

$$\mathcal{G}_{\text{offshell}}/\lambda^2 = \left(\frac{1}{2}f\rho'\rho - \frac{f\rho^2}{r}\right)\Bigg|_{r=1}^{r\to\infty} + \int_1^\infty dr\left(\frac{1}{2}\rho\hat{L}\rho + \frac{B\rho}{r^2} - \frac{J\rho^4}{4r^6}\right), \quad (14)$$

$$\mathcal{G}_{\text{offshell}}/\lambda^2 \simeq a_1(T/T_c - 1)N^2 + a_2 J N^4 - BN + \mathcal{O}(N^6), \quad (19)$$

Ising-like model:

$$\tilde{\Omega} \simeq \frac{1}{2}\left(\frac{\lambda_s\gamma_E T}{4\pi} - m_s^2\right)\tilde{s}_{cl}^2 + \frac{\lambda_s\tilde{s}_{cl}^4}{4!} + \cdots$$

arXiv: 1507.00546

on shell:

$$\mathcal{G}_{\text{onshell}} = \frac{\lambda^2}{2}\int_1^\infty dr\left(\frac{J\rho^4}{2r^6}\right) - BN,$$

where

$$N = -\frac{\lambda^2}{2}\int_1^\infty dr\frac{\rho}{r^2}.$$

Spontaneous magnetization: B=0

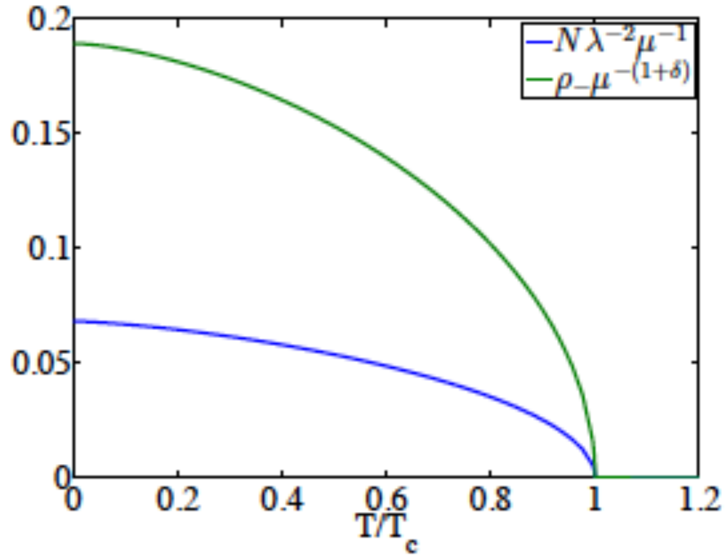

$$J = -1, m^2 = -3$$

FIG. 1. The magnetic moment as a function of temperature. Here the critical temperature is $T_c/\mu \simeq 0.00915$.

$$N^2/\lambda^4\mu^2 \simeq 6.5054 \times 10^{-3}(1 - T/T_c).$$

The response to external magnetic field:

magnetic susceptibility:

$$\chi = \lim_{B\to 0} \frac{\partial N}{\partial B}\bigg|_T .$$

$$\chi^{-1}\lambda^2/\mu \simeq 0.5463(T/T_c - 1).$$

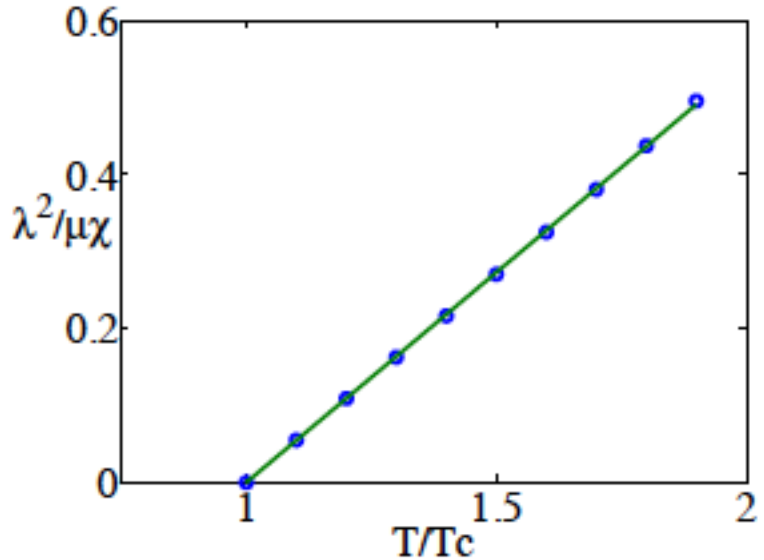

Obey the Curie-Weiss Law

The hysteresis loop in a single magnetic domain:

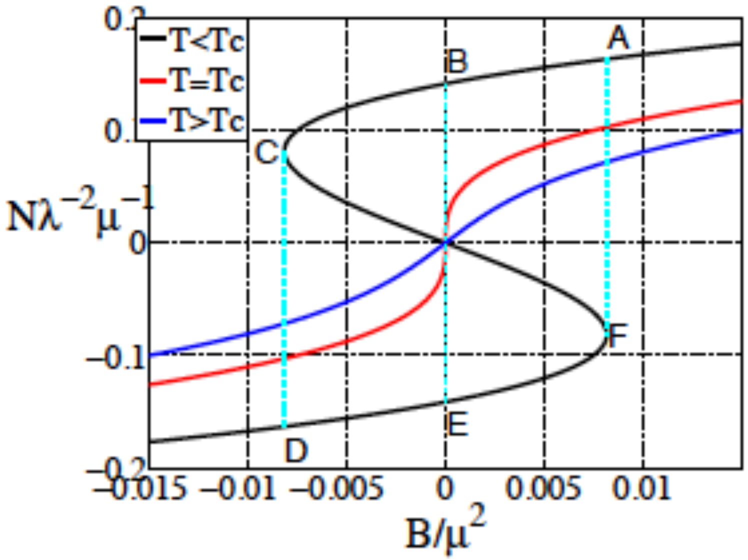

When T < Tc, the magnetic moment is not single valued. The parts DE and BA are stable, which can be realized in the external field. The part CF is unstable which cannot exist in the realistic system. The parts EF and CB are metastable states, which may exist in some intermediate processes and can be observed in experiment. When the external field continuously changes, the metastable states of magnetic moment can appear.

3、Faramagnetism/antiferromagnetism phase transition

arXiv:1404.7737

Antiferromagnetic material does not show any macroscopic magnetic moment when external magnetic field is absent, it is still a kind of magnetic ordered material when temperature is below the Neel temperature T_N. The conventional picture, due to L. Neel, represents a macroscopic antiferromagnetism as consisting of two sublattices, such that spins on one sublattice point opposite to that of the other sublattice. The order parameter is the staggered magnetization, as the diference between the two magnetic moments associated with the two sublattices:

$$\vec{M}^{\dagger} = \vec{M}_A - \vec{M}_B.$$

Three-dimensional representation of the spin alignment of manganese ions in MnF_2 [26]. The smaller spheres stand for Mn ions and larger ones stand for fluoride ions. This figure demonstrates the interpenetration of two manganese sub-lattices, Mn_1 and Mn_2, having antiparallel aligned moments.

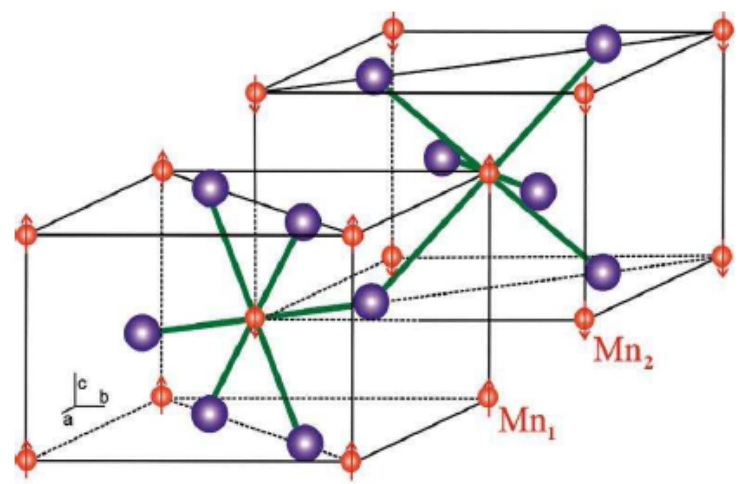

(b)

Magnetic susceptibility:

$$\chi = \frac{C}{T+\theta}, \quad T > T_N, \quad \theta > 0,$$

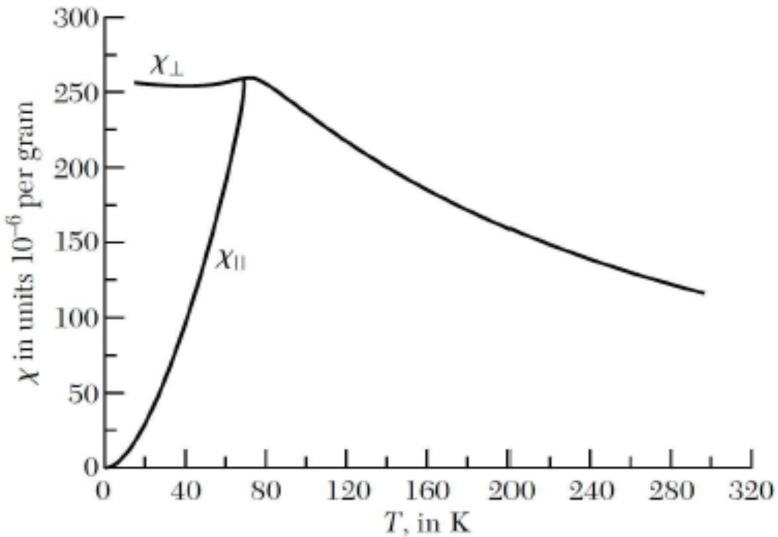

Néel temperature T_N

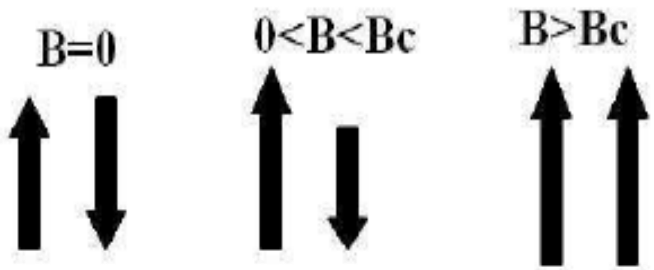

Figure 2: Left: The magnetic susceptibility of antiferromagnetic material MnF_2 [23]. $\chi_\perp$ stands for the case with external magnetic field perpendicular to the direction of spontaneous magnetization and $\chi_\parallel$ for the case with external magnetic field parallel to the direction of spontaneous magnetization. Right: The influence of external magnetic field on the magnetic moments of two sublattices when $T < T_N$.

Three minimal requirements to realize the holographic model for the phase transition of paramagnetism/antiferromagnetism.

1)The antiparallel magnetic structure as T<T_N
2)The susceptibility behavior
3)Breaking the time reversal symm & spatial rotating symm

Our model:

$$S=\frac{1}{2\kappa^2}\int d^4x\sqrt{-g}[R+6/L^2-F^{\mu\nu}F_{\mu\nu}+\lambda^2(L_1+L_2+L_{12})], \qquad (3)$$

where

$$L_{(a)}=-\frac{1}{4}\nabla^\mu M^{(a)\nu\tau}\nabla_\mu M^{(a)}_{\nu\tau}-\frac{1}{4}m^2M^{(a)\mu\nu}M^{(a)}_{\mu\nu}-\frac{1}{2}M^{(a)\mu\nu}F_{\mu\nu}-\frac{1}{8}JV(M^{(a)}_{\mu\nu})$$
$$V(M^{(a)}_{\mu\nu})=M^{(a)\mu}{}_\nu M^{(a)\nu}{}_\tau M^{(a)\tau}{}_\sigma M^{(a)\sigma}{}_\mu,\ a=1,2 \qquad (4)$$
$$L_{12}=-\frac{k}{2}M^{(1)\mu\nu}M^{(2)}_{\mu\nu},$$

The probe limit

$$ds^2 = r^2(-f(r)dt^2 + dx^2 + dy^2) + \frac{dr^2}{r^2 f(r)},$$
$$f(r) = 1 - \frac{1+\mu^2+B^2}{r^3} + \frac{\mu^2+B^2}{r^4}.$$

The ansatz:

$$M_{\mu\nu}^{(a)} = -p^{(a)}(r)dt\wedge dr + \rho^{(a)}(r)dx\wedge dy, \quad a = 1, 2.$$

Define: $$\alpha = \frac{1}{2}(\rho^{(1)} + \rho^{(2)}), \;\; \beta = \frac{1}{2}(\rho^{(1)} - \rho^{(2)}).$$

Then we can use α and β to describe the different magnetic phases. The paramagnetic, ferromagnetic, antiferromagnetic and ferrimagnetic phases correspond to the cases of $\alpha = \beta = 0$, $|\alpha| > |\beta|$, $|\alpha| = 0, \beta \neq 0$ and $0 \neq |\alpha| < |\beta|$, respectively. In the end of this paper, we will discuss the ferrimagnetic phase briefly.

The equations of motion:

$$\alpha'' + \frac{f'\alpha'}{f} + \frac{J\alpha^3}{4r^6 f} + \left(\frac{3J\beta^2}{4r^6 f} - \frac{2f'}{rf} - \frac{4}{r^2} - \frac{m^2+k}{r^2 f}\right)\alpha - \frac{2B}{r^2 f} = 0,$$
$$\beta'' + \frac{f'\beta'}{f} + \frac{J\beta^3}{4r^6 f} + \left(\frac{3J\alpha^2}{4r^6 f} - \frac{2f'}{rf} - \frac{4}{r^2} - \frac{m^2-k}{r^2 f}\right)\beta = 0.$$

The boundary conditions:

$$\alpha' = 2\alpha - \frac{J\alpha(\alpha^2+3\beta^2) - 4\alpha(m^2+k) - 8B}{16\pi T},$$
$$\beta' = 2\beta - \frac{J\beta(\beta^2+3\alpha^2) - 4\beta(m^2-k)}{16\pi T},$$

$$\alpha = \alpha_+ r^{(1+\delta_1)/2} + \alpha_- r^{(1-\delta_1)/2} - \frac{2B}{m^2+k+4},$$
$$\beta = \beta_+ r^{(1+\delta_2)/2} + \beta_- r^{(1-\delta_2)/2},$$
$$\delta_1 = \sqrt{17+4k+4m^2}, \quad \delta_2 = \sqrt{17-4k+4m^2},$$

The parameter constraint:

$$\left|\frac{3}{2}+m^2\right| < k < 4+m^2.$$

The on-shell free energy:

$$G_\rho = \lambda^2 \int_1^\infty dr \left[\frac{B\alpha}{r^2} + \frac{J(\rho^{(1)4}+\rho^{(2)4})}{4r^6}\right] = \lambda^2 \left[\int_1^\infty dr \frac{J(\alpha^4+\beta^4+6\alpha^2\beta^2)}{2r^6} - BN\right]. \quad (18)$$

Here the total magnetic moment density is defined by

$$N = N_1 + N_2 = -\lambda^2 \int_1^\infty \frac{\alpha}{r^2} dr, \quad \text{with } N_a = -\frac{\lambda^2}{2}\int_1^\infty \frac{\rho^{(a)}}{r^2} dr. \quad (19)$$

The order parameter for antiferromagnetic phase transition, i.e., the staggered magnetization, is defined as,

$$N^\dagger = N_1 - N_2 = -\lambda^2 \int_1^\infty \frac{\beta}{r^2} dr. \quad (20)$$

$$m^2 = -2, k = 1$$

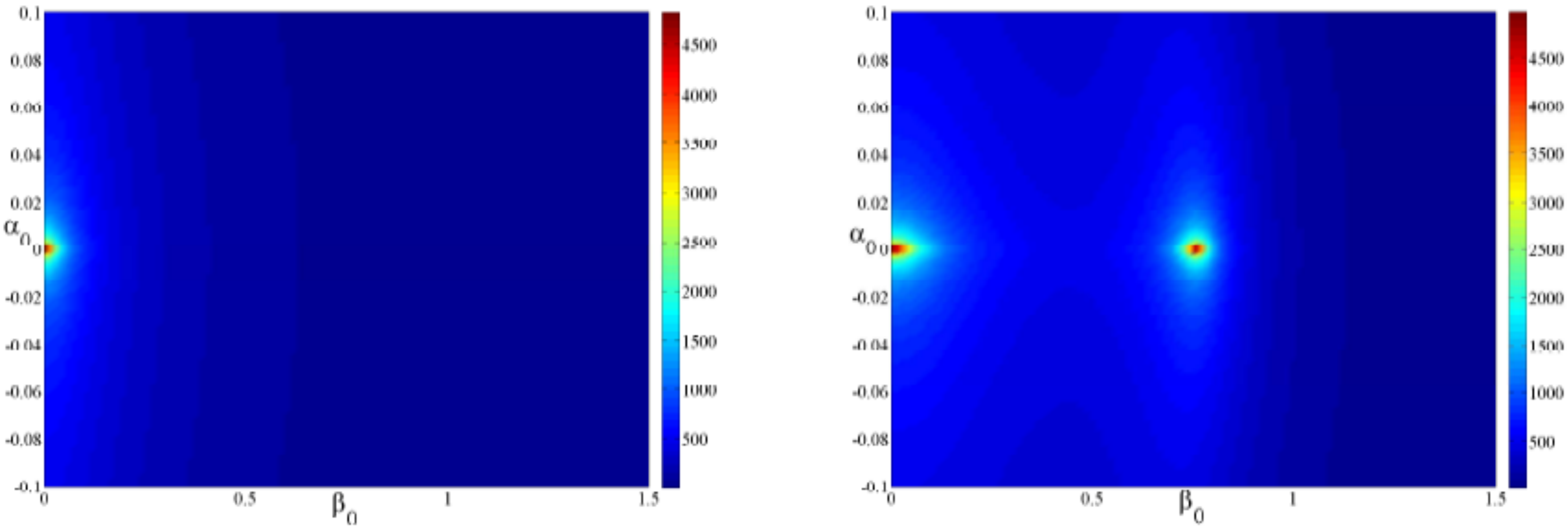

Figure 3: The value of $(\alpha_+{}^2 + \beta_+{}^2)^{-1}$ in the plane of α_0-β_0 in different temperature. Left: $T/\mu \simeq 0.0111$. Right: $T/\mu \simeq 0.0083$.

alpha_0 and beta_0 are initial values at the horizon!

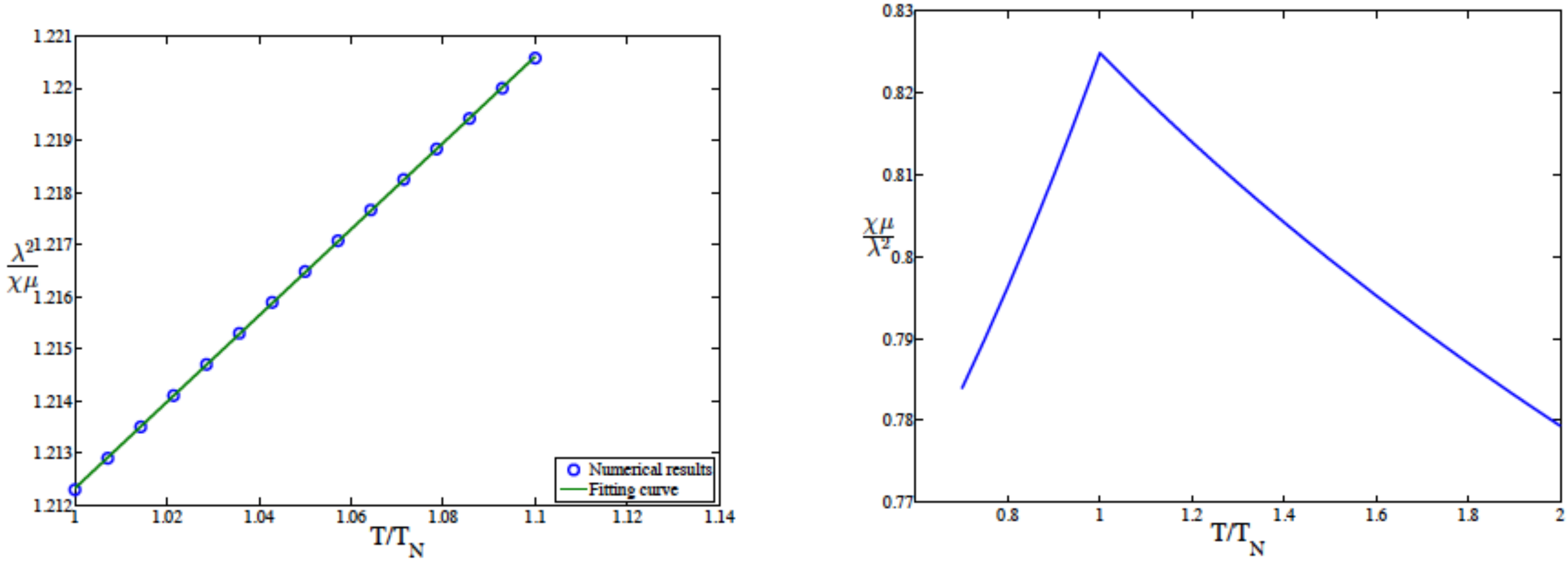

Figure 4: The susceptibility density versus the temperature. Left: The behavior of the inverse susceptibility density in the paramagnetic phase near the critical temperature. Right: The susceptibility density in the antiferromagnetic phase and paramagnetic phase.

$$\lambda^2/\mu\chi \approx 0.0827(T/T_N + 13.65),$$

$$\theta/\mu \approx 13.65T_N/\mu = 0.1263.$$

The influence on strong external magnetic field

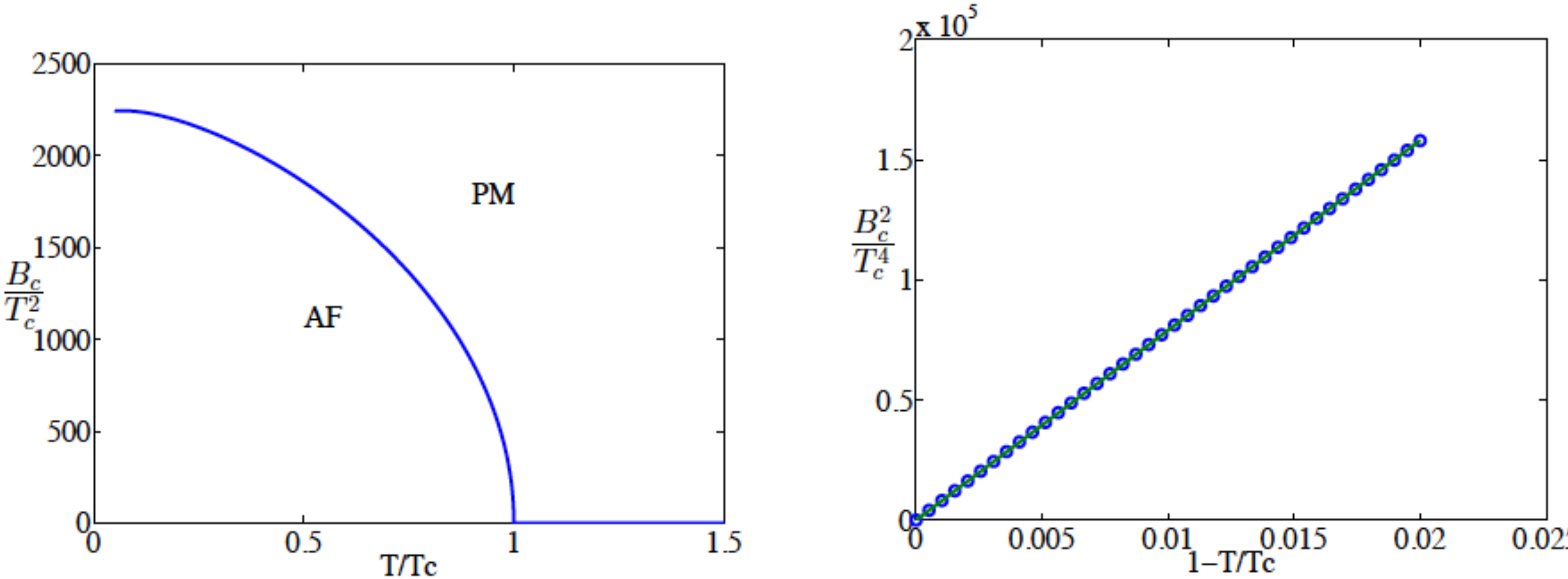

Figure 5: The critical magnetic field versus the temperature.

$$B_c^2 \simeq 7.9 \times 10^6 T_c^4 (1 - T/T_N).$$

4、Antiferromagnetic quantum phase transition

$$S=\frac{1}{2\kappa^2}\int d^4x\sqrt{-g}[R+\frac{6}{L^2}-F^{\mu\nu}F_{\mu\nu}-\lambda^2(L_1+L_2+L_{12})], \tag{1}$$

where

$$\begin{aligned} L_{12}&=\frac{k}{2}M^{(1)\mu\nu}M^{(2)}_{\mu\nu},\\ L_{(a)}&=\frac{1}{12}(dM^{(a)})^{\mu\nu\tau}(dM^{(a)})_{\mu\nu\tau}+\frac{m^2}{4}M^{(a)\mu\nu}M^{(a)}_{\mu\nu}\\ &\quad+\frac{1}{2}M^{(a)\mu\nu}F_{\mu\nu}+JV(M^{(a)}_{\mu\nu}),\\ V(M^{(a)}_{\mu\nu})&=({}^{*}M^{(a)}{}_{\mu\nu}M^{(a)\mu\nu})^2,\ a=1,2. \end{aligned} \tag{2}$$

$$\alpha=(M^{(1)}_{xy}+M^{(2)}_{xy})/2,\quad \beta=(M^{(1)}_{xy}-M^{(2)}_{xy})/2.$$

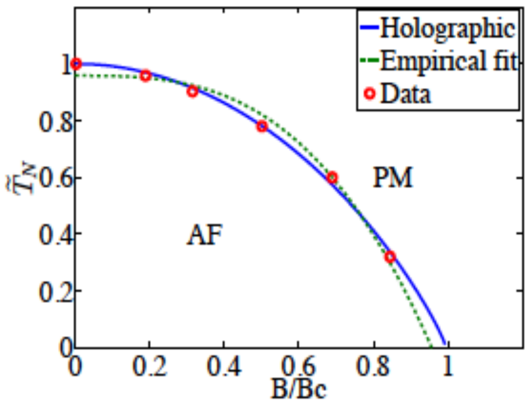

FIG. 1. The antiferromagnetic critical temperature T_N versus the external magnetic field B calculated at the model parameters $k = -m^2 = 3/2$, $J = -6$ (solid curve) and compared with experimental data from $BiCoPO_5$ (red circles) and mean field theory (green dashed line). The experimental data are from [22] and rescaled.

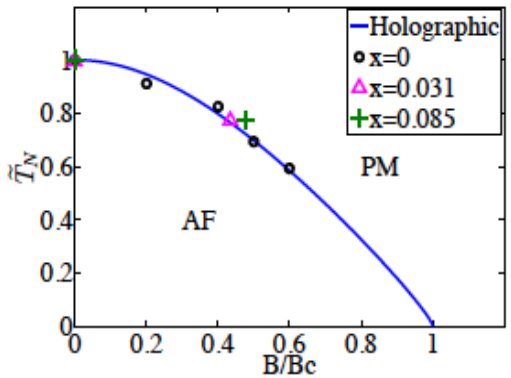

FIG. 2. The antiferromagnetic critical temperature T_N versus the external magnetic field B calculated at the model parameters $k = -m^2 = 3/2$, $J = -1$ (solid curve) and compared with experimental data for pyrochlore compounds: $Er_{2-2x}Y_{2x}Ti_2O_7$. Black circles corresponds to zero doping, $x = 0$; magenta triangulars - to $x = 0.031$; green crosses - to $x = 0.085$. The experimental data are from [23].

$$\widetilde{T}_N / \ln \widetilde{T}_N \propto (1 - B/B_c),$$

critical magnetic field

$$\widetilde{\Delta} \propto (B/B_c - 1), \text{with } \widetilde{\Delta} = \Delta/T_{N0}.$$

$$l \simeq (B/B_c - 1)^{-\nu}, \quad \text{with } \nu \simeq 1/2.$$

Ex:5.0, Th:4.

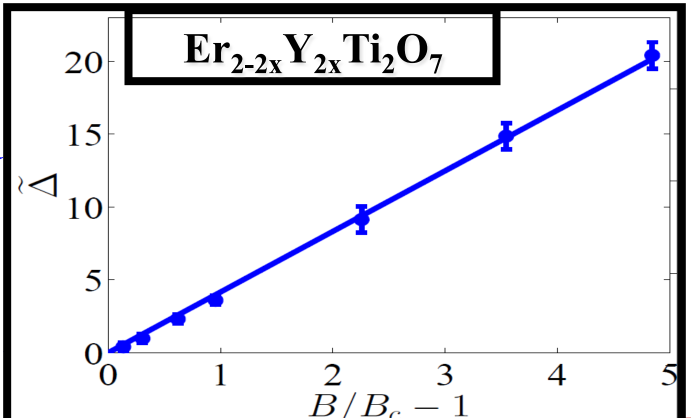

Dynamical exponent: 2

$La_{2-x}Ce_xCuO_{4\pm d}$: Current experiments from IOP

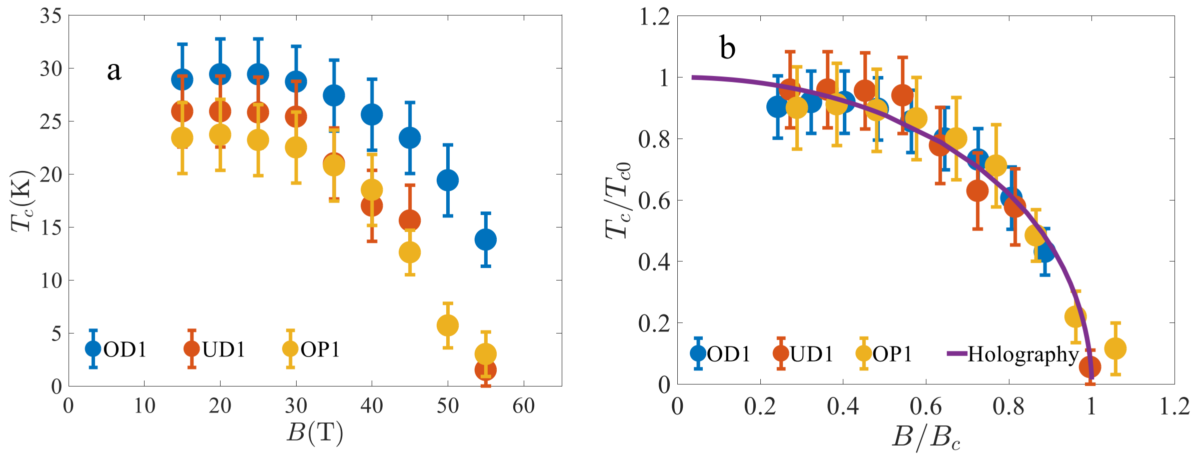

Figure. 9: (a) The relationship between AFM transition temperature T_c and external magnetic field B for three different samples. **(b)** The comparison between the experimental data and holographic prediction. The critical magnetic fields are B_c≈62T, 55.2T and 52T. The critical temperature at zero external magnetic field are $\boldsymbol{T_{c0}}$≈32K, 27K and 26K. The best fitting show k≈3.8.

The model predicts a quasi particle excitation:

$$\frac{\Delta}{k_B T_{c0}} \propto \frac{B}{B_c} - 1$$

5、Insulator/metal phase transition and colossal magnetoresistance in holographic massive gravity

Some magnetic materials such as manganites exhibit the colossal magnetoresistance effect.

Our model:

$$S = \frac{1}{16\pi G}\int d^4x\sqrt{-g}[\mathcal{R} + \frac{6}{L^2} - (L_{\text{ins}} + \lambda^2 L_{\text{ferr}}) + L_{\text{mg}}],$$

$$L_{\text{ins}} = e^{-2g_0\psi}F_{\mu\nu}F^{\mu\nu} + \frac{1}{2}(\nabla\psi)^2 + \frac{m_2^2}{2}\psi^2,$$

$$L_{\text{ferr}} = \frac{(dM)^2}{12} + \frac{m_1^2}{4}M_{\mu\nu}M^{\mu\nu} + \frac{1}{2}M^{\mu\nu}F_{\mu\nu} + \frac{J}{8}V(M),$$

$$L_{\text{mg}} = \alpha\text{Tr}\mathcal{K} + \beta[(\text{Tr}\mathcal{K})^2 - \text{Tr}\mathcal{K}^2],$$

$$\mathcal{K}^{\mu}{}_{\nu}\mathcal{K}^{\nu}{}_{\tau} = g^{\mu\nu}\mathfrak{f}_{\nu\tau}$$

$$V(M) = ({}^*M_{\mu\nu}M^{\mu\nu})^2 = [{}^*(M\wedge M)]^2.$$

Blake, Tong and Vegh, arXiv:1310.3832
Blake and Tong, arXiv:1308.4970
Mefford and Horowitz, arXiv: 1406.4188

There is a position dependent mass

$$m_g^2(r) = -2\beta - \alpha/r.$$

This measures the strength of inhomogeneity

The black brane solution:

$$ds^2 = -r^2 f e^{-\chi} dt^2 + \frac{dr^2}{r^2 f} + r^2(dx^2 + dy^2),$$

The ansatz:

$$A_\mu = \phi(r)dt + Bxdy, \;\; \psi = \psi(r),$$
$$M_{\mu\nu} = -p(r)dt \wedge dr + \rho(r)dx \wedge dy.$$

The asymptotic solution at the boundary:

$$\rho = \rho_+ (\frac{r}{r_h})^{(1+\delta_1)/2} + \rho_- (\frac{r}{r_h})^{(1-\delta_1)/2} + \cdots + \frac{B}{m_1^2},$$
$$p = \frac{\sigma r_h^2}{m_1^2 r^2} + \cdots\,, \;\; \phi = \mu - \frac{\sigma r_h}{r} + \cdots\,,$$
$$\psi = \psi_+ (\frac{r}{r_h})^{(\delta_2 - 3)/2} + \psi_- (\frac{r}{r_h})^{-(\delta_2+3)/2} + \cdots\,,$$

$$\delta_1 = \sqrt{1 + 4m_1^2} \text{ and } \delta_2 = \sqrt{9 + 4m_2^2},$$

DC conductivity:

The perturbation: $\delta A_x = \epsilon a_x(r) e^{-i\omega t}$

we have following equations in the low frequency limit,

$$C_{ty}'' + \frac{1}{2}\chi' C_{ty}' - \frac{m_1^2 C_{ty}}{r^2 f} - \frac{4Jp\rho C_{rx}}{r^2} + O(\omega) = 0, \quad (9a)$$

$$m_1^2 C_{rx} - a_x' - \frac{4Je^{\chi} p\rho C_{ty}}{r^4 f} + O(\omega) = 0, \quad (9b)$$

$$[r^2 f e^{-\chi/2}(e^{-2g_0\psi} a_x' - \lambda^2 C_{rx}/4)]' + O(\omega) = 0, \quad (9c)$$

The AdS boundary:

$$a_x = a_{x+} + \frac{a_{x-}}{r} + \cdots .$$

$$\langle J \rangle = a_{x-}$$

DC resistivity:

$$R = \lim_{\omega\to 0} i\omega a_{x+}/\langle J\rangle.$$

By the membrane paradigm:

Iqbal and Liu, arXiv: 0809.3808

$$\langle J\rangle = \frac{i\omega a_x(r_h)}{1-\frac{\lambda^2}{4m_1^2}}\left[e^{-2g_0\psi_0} - \frac{\lambda^2 m_1^2}{4(m_1^4+16J^2e^{\chi_0}p_0^2\rho_0^2/r_h^4)}\right].$$

The DC resistivity in the strong inhomogeneity limit:

$$\frac{1}{R_{\text{heavy}}} =(1-\frac{\lambda^2}{4m_1^2})^{-1}\left[e^{-2g_0\psi_0} - \frac{\lambda^2 m_1^2}{4(m_1^4+16J^2e^{\chi_0}p_0^2\rho_0^2/r_h^4)}\right] + \mathcal{O}(1/m_g^2),$$

Numerical results: $m_1^2 = 1/3, m_2^2 = -2, m_g^2 = 40, g_0 = 1$ and $\lambda = 3/4$

$\mathrm{MR}(B) = 1 - R(B)/R(B=0) \propto \rho_0^2 \propto B^2.$

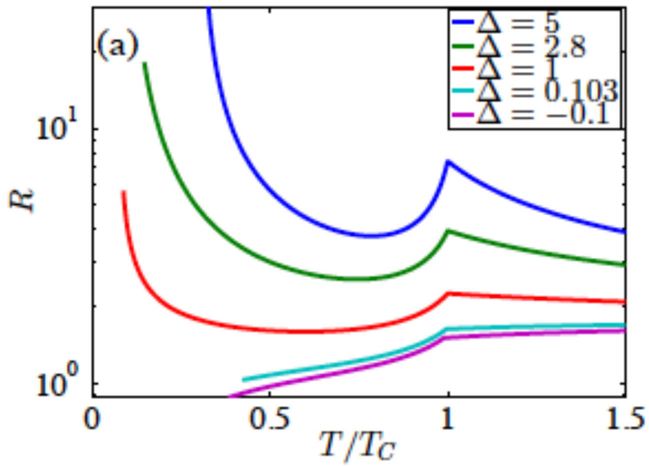

$B = 0$ and $J = -2.$

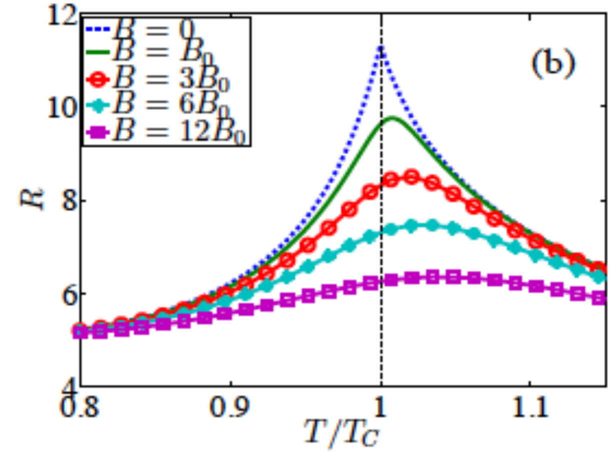

$B_0/T_C^2 \simeq 5.5 \times 10^{-4}$, and $J = -1/3.$

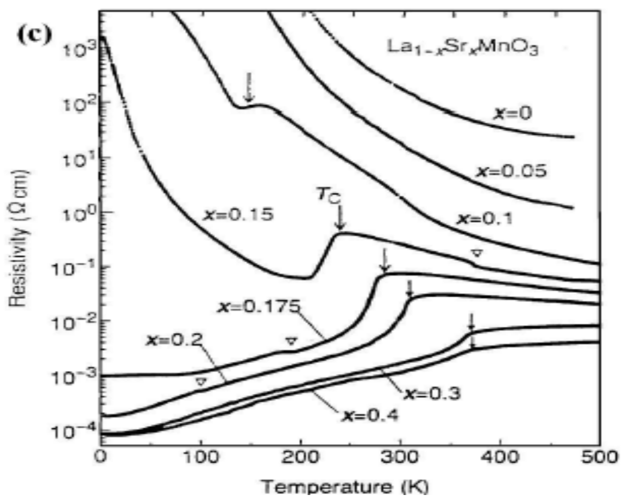

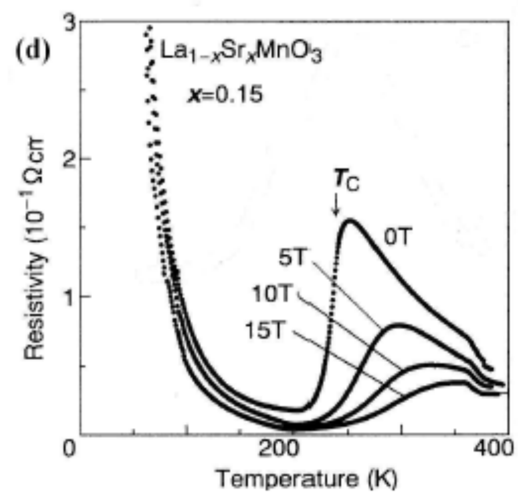

A. Urushibara et al, PRB51 (1995)

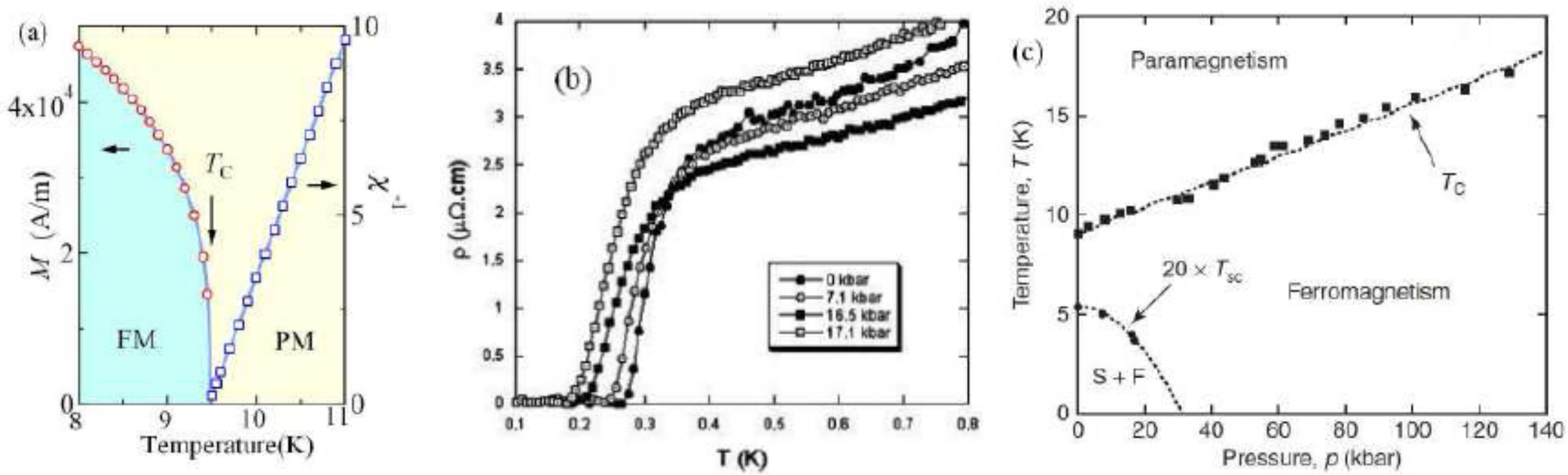

Figure 1: The experimental results on the p-wave superconducting ferromagnetic material URhGe. **(a)** Temperature dependence of the spontaneous magnetization $M(T)$ and the inverse of the magnetic susceptibility $\chi^{-1}(T)$ under the normal pressure [6]. **(b)**Temperature dependence of the resistivity of URhGe for different pressures at low temperature. The superconducting critical temperature is defined by the zero resistivity point [7]. **(c)** Pressure-temperature phase diagram of URhGe [7].

6、Coexistence between ferromagnetism and p-wave order

（arXiv:1410.5080)

P-wave: Einstein-Maxwell-Complex vector model:

$$S = \frac{1}{2\kappa^2}\int d^4x\sqrt{-g}(\mathcal{R} + \frac{6}{L^2} + \mathcal{L}_m),$$

$$\mathcal{L}_m = -\frac{1}{4}F_{\mu\nu}F^{\mu\nu} - \frac{1}{2}\rho^\dagger_{\mu\nu}\rho^{\mu\nu} - m^2\rho^\dagger_\mu\rho^\mu + iq\gamma\rho_\mu\rho^\dagger_\nu F^{\mu\nu},$$

arXiv: 1309.4877, JHEP 1401 (2014) 032

Our model:

$$S = \frac{1}{2\kappa^2}\int d^4x\sqrt{-g}\left[R + \frac{6}{L^2} - F_{\mu\nu}F^{\mu\nu} + \mathcal{L}_\rho + \mathcal{L}_M + \mathcal{L}_{\rho M}\right],$$

$$\mathcal{L}_\rho = -\frac{1}{2}\rho^\dagger_{\mu\nu}\rho^{\mu\nu} - m_1^2\rho^\dagger_\mu\rho^\mu + iq\gamma\rho_\mu\rho^\dagger_\nu F^{\mu\nu} - V_\rho,$$

$$\mathcal{L}_M = -\frac{1}{4}\nabla^\mu M^{\nu\tau}\nabla_\mu M_{\nu\tau} - \frac{m_2^2}{4}M^{\mu\nu}M_{\mu\nu} - \frac{\lambda}{2}M^{\mu\nu}F_{\mu\nu} - V_M,$$

$$\mathcal{L}_{\rho M} = -i\alpha\rho_\mu\rho^\dagger_\nu M^{\mu\nu},$$

$$V_M = \frac{J}{8}M_\mu{}^\nu M_\nu{}^\tau M_\tau{}^\delta M_\delta{}^\mu \qquad \boxed{V_\rho = -\frac{\Theta}{2}\rho_{[\mu}\rho^\dagger_{\nu]}\rho^\mu\rho^{\dagger\nu}.}$$

plays a crucial role

Conclusions:

1) In the case that the ferromagnetic phase appears first, if the interaction is attractive, the system shows the ferromagnetism and superconductivity can coexist in low temperatures. If the interaction is repulsive, the system will only be in a pure ferromagnetic state.

2) In the case that the superconducting phase appears first, the attractive interaction will lead to a magnetic p-wave superconducting phase in low temperatures. If the interaction is repulsive, the system will be in a pure p-wave superconducting phase or ferromagnetic phase when the temperature is lowered.

8) Intertwined order and holography: the case of the parity breaking pair density wave, R.G. Cai, L. Li, Y.Q. Wang and J. Zaanen, arXiv: 1706.01470, PRL119 (2017) 1181601

We present a minimal bottom-up extension of the Chern-Simons bulk action for holographic translational symmetry breaking that naturally gives rise to pair density waves. We construct stationary inhomogeneous black hole solutions in which both the U(1) symmetry and spatially translational symmetry are spontaneously broken at finite temperature and charge density. This novel solution provides a dual description of a superconducting phase intertwined with charge, current and parity orders.

LETTERS

PUBLISHED ONLINE: 21 NOVEMBER 2016 | DOI: 10.1038/NPHYS3962

nature physics

A global inversion-symmetry-broken phase inside the pseudogap region of $YBa_2Cu_3O_y$

L. Zhao[1,2], C. A. Belvin[3], R. Liang[4,5], D. A. Bonn[4,5], W. N. Hardy[4,5], N. P. Armitage[6] and D. Hsieh[1,2*]

The model:

$$S=\int d^4x\sqrt{-g}\Big[\mathcal{R}+6-\frac{1}{2}\partial_\mu\chi\partial^\mu\chi-\mathcal{F}(\chi)(\partial_\mu\theta-A_\mu)^2 \\ -\frac{Z(\chi)}{4}F^2-V(\chi)-\vartheta(\chi)\epsilon_{\mu\nu\lambda\sigma}F^{\mu\nu}F^{\lambda\sigma}\Big]. \quad (1)$$

Vacuum solution:

$$ds^2=\frac{1}{z^2}\left[-H(z)dt^2+\frac{1}{H(z)}dz^2+(dx^2+dy^2)\right], \quad (3)$$

$$H(z)=(1-z)\left(1+z+z^2-\frac{\mu^2z^3}{4}\right), \; A_t=\mu(1-z),$$

RGC and Y.Z. Zhang, PRD 54 （1996）

Topology of black hole horizon（S.Hawking,1972):

PHYSICAL REVIEW D VOLUME 54, NUMBER 8 15 OCTOBER 1996

Black plane solutions in four-dimensional spacetimes

Rong-Gen Cai* and Yuan-Zhong Zhang
China Center of Advanced Science and Technology (World Laboratory), P.O. Box 8730, Beijing 100080, China
and Institute of Theoretical Physics, Academia Sinica, P.O. Box 2735, Beijing 100080, China
(Received 7 June 1996)

The static, plane symmetric solutions and cylindrically symmetric solutions of Einstein-Maxwell equations with a negative cosmological constant are investigated. These black configurations are asymptotically anti–de Sitter–type not only in the transverse directions, but also in the membrane or string directions. Their causal structure is similar to that of Reissner-Nordström black holes, but their Hawking temperature goes with $M^{1/3}$, where M is the ADM mass density. We also discuss the static plane solutions in Einstein-Maxwell-dilaton gravity with a Liouville-type dilaton potential. The presence of the dilaton field changes drastically the structure of solutions. They are asymptotically "anti–de Sitter–" or "de Sitter-type" depending on the parameters in the theory. [S0556-2821(96)03820-9]

PACS number(s): 04.20.Jb, 04.70.Dy

$$ds^2 = -A(r)dt^2 + B(r)dr^2 + C(r)(dx^2 + dy^2), \qquad (8)$$

$$A(r) = B^{-1}(r) = \alpha^2 r^2 - \frac{m}{r} + \frac{q^2}{r^2},$$
$$C(r) = \alpha^2 r^2,$$

In this work:

$$Z(\chi) = \frac{1}{\cosh(\sqrt{3}\chi)}\,, \qquad V(\chi) = 1 - \cosh(\sqrt{2}\chi)\,,$$
$$\mathcal{F}(\chi) = \cosh(\chi) - 1\,, \quad \vartheta(\chi) = \frac{1}{4\sqrt{3}}\tanh(\sqrt{3}\chi)\,.$$

In this case, the operator dual to \chi has dimension 2.

- For the uni-directional "striped" solution:

$$\begin{aligned} ds^2 =& \frac{1}{z^2}\Big[-H(z)U_1 dt^2 + \frac{U_2}{H(z)}dz^2 + U_3(dx + z^2 U_5 dz)^2 \\ &+U_4(dy + (1-z)U_6 dt)^2\Big]\,, \qquad (4) \\ A =& A_t\, dt + A_y\, dy\,, \quad \chi = z\,\psi\,, \end{aligned}$$

Nine functions depend on z and x

- For the tetragonal case, 15 PDEs with variables z, x and y

Condensate, charge modulation and current:

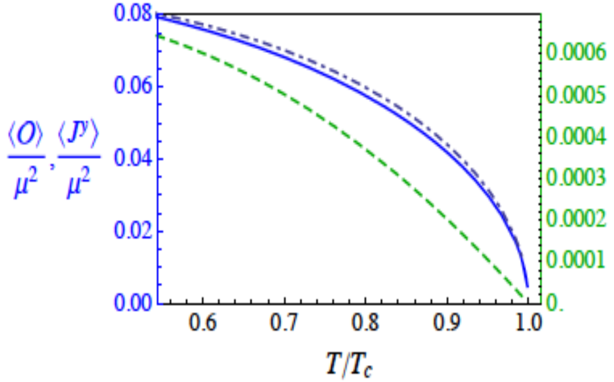

(b)

FIG. 1. (a) The stability "dome" (blue line) following from linear stability analysis in the temperature (T/μ) – ordering wave vector (k/μ) plane (μ is the chemical potential) for the unidirectional order. The actual second order transition is associated with the maximal T_c and the red dotted line shows the temperature dependence of the ordering wave vector of the fully back-reacted "intertwined" order. (b) The temperature dependence of the charge modulation $\Delta\rho$ (dashed), current $\langle J^y \rangle$ (dash-dotted) and pair density wave $\langle O \rangle$ (full line) VEV's of the uni-directional phase. The dominating current and pair density wave VEV's show a characteristic mean field temperature evolution, while the "parasitic" charge density modulation $\Delta\rho$ increases linearly. Non-trivial configurations of $\langle O \rangle$ also imply a spontaneous breaking of parity, which was very recently observed in the cuprates [6]. Similar results are obtained for the full tetragonal order of Fig. 2.

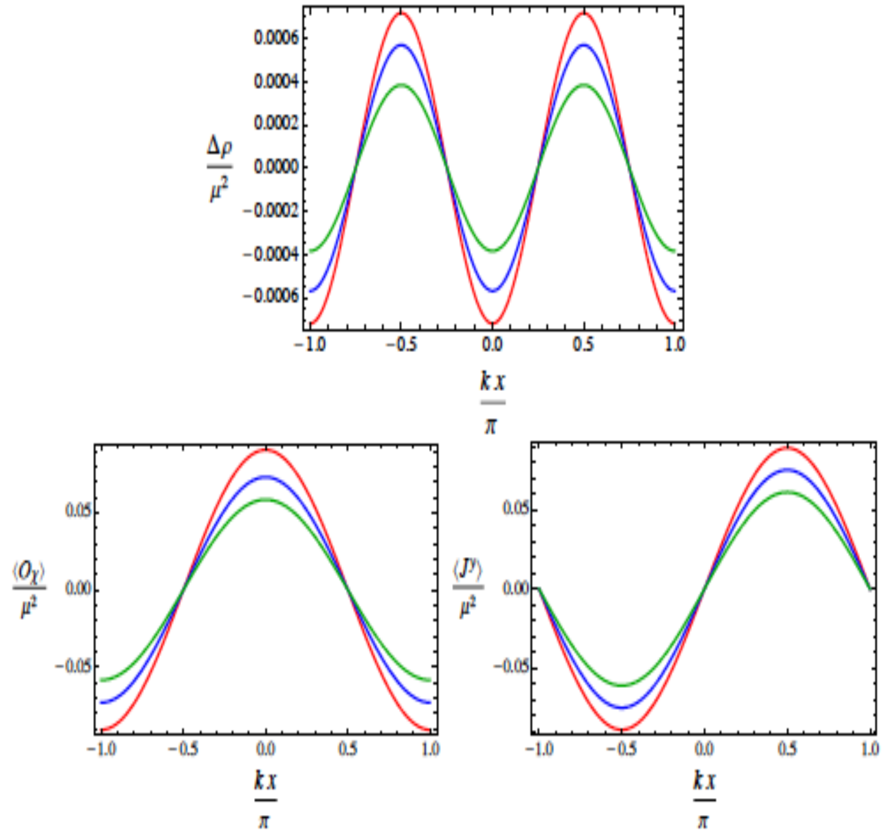

FIG. 3. The modulation of charge density (up), scalar condensate (bottom left) and current order (bottom right). We consider the $k = k_c$ branch with $T/T_c \approx$ 0.0828 (red), 0.640 (blue), 0.792 (green) from top to down for each plot.

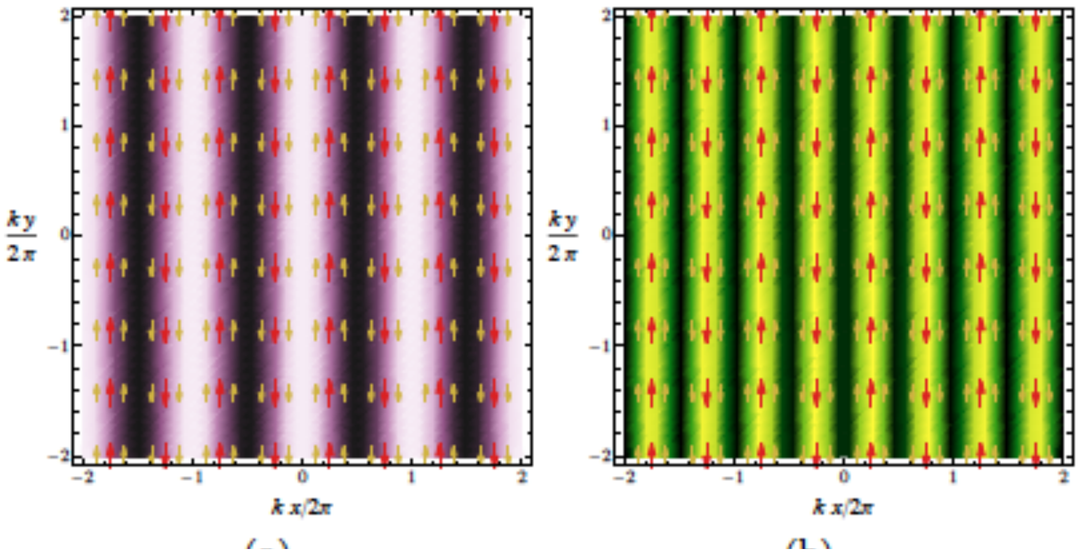

FIG. 2. The density plots of (a) condensate and (b) charge density distribution for uni-directional phase at $T/T_c \approx 0.64$,

The arrows denote integral curves of the currents $(\langle J^x\rangle, \langle J^y\rangle)$. The bright parts correspond to large positive values while the dark region to the negative values. In the uni-directional phase the charge density oscillates at twice the frequency of the currents and condensate.

The density plots of (c) condensate and (d) charge density distributions

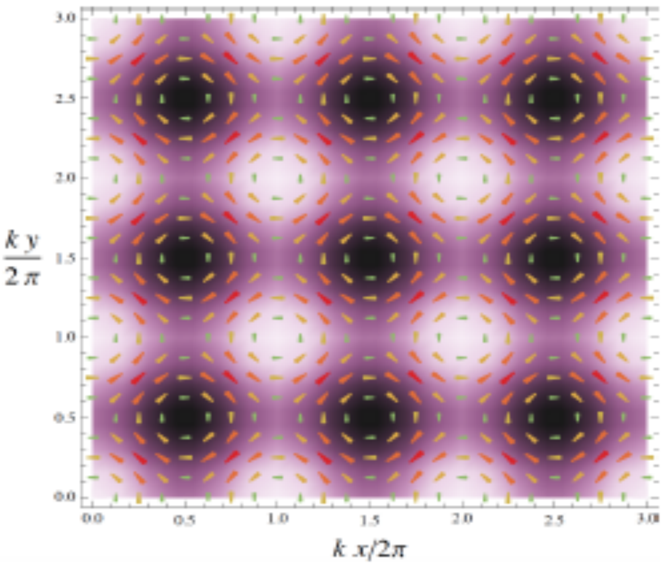

(c)

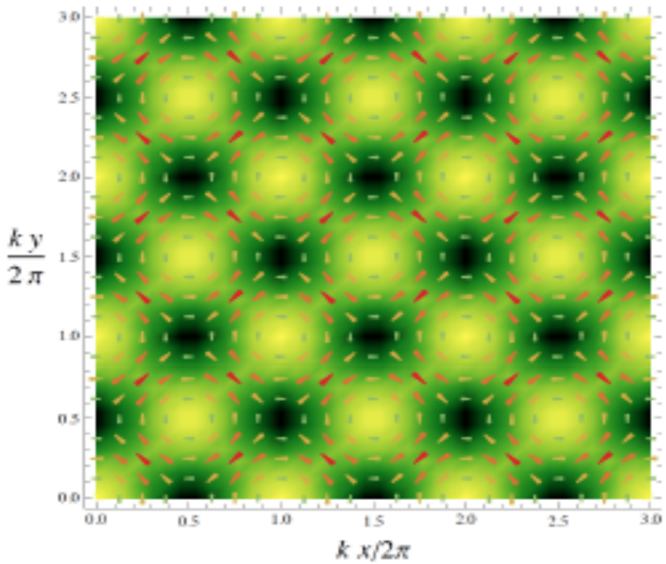

(d)

for the square checkerboard at $T/T_c \approx 0.94$. The arrows denote integral curves of the currents $(\langle J^x \rangle, \langle J^y \rangle)$. The bright parts correspond to large positive values while the dark region to the negative values. In the uni-directional phase the charge density oscillates at twice the frequency of the currents and condensate. The latter two orders are precisely out-of phase. The checkerboard is a tetragonal charge crystal going hand in hand with a staggered pattern of current fluxes circling around the plaquettes, which is similar to the d-density waves of condensed matter physics.

8、Summary

1) present a holographic model for the paramagnetism -ferromagnetism phase transition
2) realize the paramagnetism−antiferromagnetism transition
3) antiferromagnetic quantum phase transition
4） insulator/metal phase transition and colossal magnetoresistance effect
5) coexistence and competition between ferromagnetism and p-wave superconductivity
6) Holographic model for the pair density wave

Thanks !